Harms, E, Stoetzer, C, Stueber, T, O'Reilly, AO and Leffler, A

Investigation into the role of an extracellular loop in mediating proton-evoked inhibition of voltage-gated sodium channels

Investigation into the role of an extracellular loop in mediating proton-evoked inhibition of voltage-gated sodium channels

Carsten Stoetzer[1], Elisa Harms[1], Thomas Stueber[1], Andrias O. O´Reilly[2], Andreas Leffler[1]

1. Department of Anesthesiology and Intensive Care Medicine, Hannover Medical School, Hannover, Germany.
2. School of Natural Sciences and Psychology, Liverpool John Moores University, United Kingdom.

Corresponding author:

Andreas Leffler

Department of Anesthesiology and Intensive Care Medicine

Carl-Neuberg-Strasse 1, 30625 Hannover, Germany

Tel.: ++49 (0) 511 532 3484, Fax: ++49 (0) 511 532 3642

E-mail: leffler.andreas@mh-hannover.de

Abstract

Proton-evoked activation of sensory neurons is counteracted by inhibition of voltage-gated Na+ channels, and the low acid-sensitivity of sensory neuron of the African naked mole-rat (ANMr) was reported to be due to a strong proton-evoked block of ANMrNav1.7. Here we aimed to reevaluate the role of the suggested negativelycharged motif in the ANMrNav1.7 domain IV P-loop for inhibition by protons. Patch clamp recordings were performed on the recombinant α-subunits Nav1.2–1.8. The insertion of the negatively charged motif (EKE) of ANMrNav1.7 into human Nav1.7 results in an increased proton-evoked tonic inhibition, but also in a reduced channel function. While the voltage-dependency of fast inactivation is changed in hNav1.7-EKE, pH 6.4 fails to induce a significant shift in both constructs. Proton-evoked inhibition of other channel α-subunits reveals a discrete differential inhibition among α-subunits with hNav1.7 displaying the lowest proton-sensitivity. The mutant hNav1.7-EKE displays a similar proton-sensitivity as Nav1.2, Nav1.3, Nav1.6 and Nav1.8. Overall, a correlation between proton-evoked inhibition and motif charge was not evident. Accordingly, a homology model of hNav1.7 shows that the EKE motif residues do not contribute to the pore lumen. Our data confirms that a negative charge of a postulated proton-motif encodes for a high proton-sensitivity when inserted into hNav1.7. However, a negatively charged motif is not a reliable predictor for a high proton-sensitivity in other α-subunits. Given the distance of the proton-motif from the pore mouth it seems unlikely that a blocking mechanism involving direct obstruction of the pore underlies the observed proton-evoked channel inhibition

Introduction

Voltage-gated Na+ channels (VGSC) are crucial for action potential generation in most excitable cells. In peripheral nociceptive sensory neurons, excitability seems to be finely orchestrated by several VGSC αsubunits including Nav1.1, Nav1.3, Nav1.6, Nav1.7, Nav1.8 and Nav1.9 [15]. While all of these α-subunits have been shown to carry out specialized and partially non-overlapping functions in nociceptors leading to certain types of pain, the tetrodotoxin-sensitive α-subunit Nav1.7 have emerged as a key determinant for peripheral pain signaling [3]. Human subjects carrying inherited non-functional variants of Nav1.7 never experienced the sensation of pain, whereas several gain-of-function mutations of Nav1.7 results in chronic pain syndromes [5]. Thus Nav1.7 is required for intact pain sensitivity in both rodents and humans, and an inhibition of Nav1.7 likely results in pain reduction.

Tissue acidosis develops in course of inflammation as well as ischemia, and high concentrations of protons are known to evoke pain by activating ion channels such as TRPV1, TRPA1 and acid sensing ion channels (ASICs) in sensory neurons resulting in inflammatory pain or ischemic pain [2,6,10]. Conversely, protons are also known to directly inhibit VSGCs in a concentration-dependent manner [7,13,14]. Hence, acid-evoked activation of sensory neurons and resulting pain seems to be counteracted by a concomitant reduction of Na+ currents which are required for the generation and propagation of action potentials. Saying this however, there is a remarkable scarcity of reports which explored the effects of protons on VGSCs expressed in sensory neurons. In cultured trigeminal ganglion neurons, Nakamura and colleagues reported that acid inhibits tetrodotoxin-resistant Na+ currents more strongly than tetrodotoxin-sensitive currents [13,14]. Whether or not this difference is due to differential acid-evoked block of specific α-subunits however, was not yet studied. Thus, the properties and relevance of proton-evoked block of the tetrodotoxin-sensitive α-subunit Nav1.7 in mammalian sensory neurons remain to be elucidated. However, tt has been suggested that the failure of protons to robustly activate sensory neurons from the African naked mole-rat (ANMr) is due to a potent proton-evoked block of ANMrNav1.7

[18]. As the ANMr lives underground under conditions of high CO_2 that produces tissue acidosis, it was suggested that the Nav1.7-dependent proton-evoked block of sensory neurons enables ANMr to live at such conditions without suffering from acid-evoked pain. When comparing ANMrNav1.7 with the less proton-sensitive human Nav1.7 orthologue, Smith and colleagues proposed that the amino acids EKE (position 1718–1720) in the domain IV S5–S6 extracellular linker of ANMrNav1.7 are likely to form a negatively-charged motif for protons [18]. In hNav1.7 the corresponding motif carries a 2-fold positive charge (KKV, i.e.++ 0), and the insertion of the EKE-motif into hNav1.7 indeed resulted in a strongly potentiated proton-evoked block. While the original report of Smith and colleagues was highly recognized at the time of publication, the finding has not been further pursued or even confirmed in later studies. In the present in vitro study on recombinant α-subunits, we therefore asked if the mutant construct hNav1.7-EKE containing the suggested motif for protons in ANMrNav1.7 indeed displays an increased proton-evoked block as compared to wildtype hNav1.7 We also explored to what extent protons differentially inhibit mammalian orthologues of the α-subunits Nav1.2, Nav1.2, Nav1.3, Nav1.4, Nav1.5, Nav1.6, Nav1.7 and Nav1.8, and if this differential block correlate with the charge of the proposed motif for protons.

Material and methods

2.1. Transfection and cell culture

Human-embryonic-kidney cells stably expressing rat Nav1.2, rat Nav1.3, rat Nav1.4 and human Nav1.5 were grown under standard cellculture conditions with 5% CO2 at 37 °C in Dulbecco's modified Eagle medium (DMEM, GIBCO-Invitrogen, Germany) supplemented with 10% heat-inactivated fetal bovine serum (FBS, Biochrom, Germany), 1% penicillin/streptomycin (GIBCO-Invitrogen, Germany). We added 1% G418 for stable expression of Nav1.2 and Nav1.3 and 0.4% zeocin (GIBCO-Invitrogen, Germany) for Nav1.5 to the medium. For Nav1.4 the medium was supplemented with 2% G418. Transient transfections for human Nav1.6 and Nav1.7 as well as rat Nav1.8 were performed using the nanofectin transfection kit as described previously [19]. The mutant construct hNav1.7-EKE was generated by site directed mutagenesis of hNav1.7 cDNA using the quikchange lightning site-directed mutagenesis kit (Agilent, Waldbronn, Germany) according to the instructions of the manufacturer. The mutant was subsequently sequenced to verify intended amino acid exchanges, and to exclude further channel mutation. Nav1.6 and Nav1.8 express poorly in HEK-cells and were therefore examined in the neuroblastoma-cell line N1E115. As these cells express endogenous sodium channels, the experiments on Nav1.6 and Nav1.8 were performed in presence of 300 nM tetrodotoxin. While wildtype Nav1.6 is tetrodotoxin-sensitive, we used a mutant Nav1.6 construct being tetrodotoxin-resistant (a generous gift from Angelika Lampert, Aachen). Neuroblastoma N1E115 cells were cultured in DMEM supplemented with 10% FBS (Biochrom, Germany), penicillin/streptomycin (1%, GIBCO-Invitrogen). Plasmid encoding green-fluorescent-protein was co-transfected for the purpose of visualizing transfected cells. Transfected cells were used within 2 days.

2.2. Solutions

We performed whole-cell patch clamp recordings with an extracellular solution consisting (mmol/l): 140 NaCl, 3 KCl, 1 CaCl2, 1 MgCl2, 1 CaCl2 and 10 HEPES (or 10 MES fo acidic solutions). The pHvalue was adjusted the desired pH-values with HCl or TMA-OH. For recordings of Nav1.6 and Nav1.8, 300 nM tetrodotoxin (TTX, Alomone labs, Jerusalem, Israel) was included in all solutions in order to block all endogenous TTX-sensitive Na+ channels expressed in N1E115 cells. For the experiments we replaced the medium of the cell culture dishes with the extracellular solution (pH 7.4) and applied the test-solutions in increasing pH-values using a self-made, gravity driven application system. The pipette solution contained (mmol/l): 140 CsF, 10 NaCl, 1 EGTA, 10 HEPES. The pH-value was adjusted to 7.4 with CsOH. All solutions were stored at 7 °C in light-excluding bottles and used within one month.

2.3. Patch clamp technique and data acquisition

All experiments were performed at room temperature utilizing an EPC10 amplifier (HEKA Instruments Inc., NY, U.S.A.). We prepared and heat polished patch pipettes from glass capillaries (Science Products, Hofheim, Germany) on a micropipette puller system P-1000 (Sutter Instrument, Novato, U.S.A.) to give a resistance of 1.8-2.3 MΩ when filled with pipette solution. The series resistance was minimized by compensation of the series resistance in a range between 60 and 80% and capacitance artefacts were eliminated using the amplifier circuitry. Except for use-dependent block, linear leak subtraction based on resistance estimates from four hyperpolarizing pulses applied before the test pulse, was used for all voltage-clamp recordings, and currents were filtered at 5 kHz. We used the Patchmaster v20 × 60 software (HEKA Instruments Inc., NY, U.S.A.) for recording of the experiments, the Pulse and Pulse Fit software (HEKA Instruments Inc., NY, USA) for analysis and Origin 7.0 (Microcal Software,v Northampton, MA) for statistical analysis and curve fitting. The half-maximal effective concentration (IC50) was evaluated by normalizing the peak currents amplitudes at each drug concentration value achieved in control solution. Data were fitted

with Hill equation (y = ymax * (IV50n/IC50n * Cn), where ymax is the maximal amplitude, IC50 the concentration at which y/ ymax = 0.5, and n is the Hill coefficient). To investigate the inactivation curves, peak currents evoked by a test pulse were measured, normalized and plotted against the conditioning pre-pulse potential.

2.4. Statistical analyses

Statistics were calculated using Origin 8.5 (Microcal Software,v Northampton, MA). Multiple comparisons for groups with equal, balanced sample sizes were performed by ANOVA with a Tukey post hoc test. If appropriate, single comparisons of independent groups of data were calculated with the unpaired t-test. Significance was assumed for $p < 0.05$. All data were presented as mean ± S.E.M.

2.5. Homology modeling

A homology model of hNav1.7 (UniProt accession Q15858) was generated using the 3.8 Å resolution structure of the Periplaneta americana sodium channel NavPaS (PDB code 5 × 0 M) [16]. Sequences were aligned using Clustal Omega [17]. 50 starting models were generated using MODELLER [4]. The internal scoring function of MOD ELLER was used to select 10 models, which were visually inspected and submitted to the VADAR webserver [21] to assess stereochemistry in order to select the best final model. Figures were produced using ALINE [1] and PyMOL (DeLano Scientific, San Carlos, CA, USA).

Results

3.1. Proton-evoked inhibition is enhanced in the hNav1.7-EKE mutant

We first examined tonic inhibition of wildtype hNav1.7 and the mutant hNav1.7-EKE by protons. Cells were held at −120 mV and 10 ms long test pulses to 0 mV were applied every 10 s. As is demonstrated in Fig. 1A and B, protons evoked a concentration-dependent block of both wildtype hNav1.7 (A) and the hNav1.7-EKE mutant (B). The resulting Ki values as calculated by the Hill equation gave pH 5.8 ± 0.05 (Hill coefficient 1.1 ± 0.06, n = 8) for wildtype, and 6.2 ± 0.1 (Hill coefficient 1.1 ± 0.04; n = 8) for hNav1.7-EKE (Fig. 1C). Although these data indicate that hNav1.7-EKE is indeed more strongly blocked by protons as compared to wildtype hNav1.7, the difference did not reach statistical significance ($p = 0.054$, unpaired t-test). In the original report from Smith and colleagues however, the increased proton-sensitivity of hNav1.7-EKE was verified due to inhibition only by pH 6.0. When we compared the degree of block by pH 6.0 in our experiments, we indeed obtained a significantly stronger block by pH 6.0 of hNav17-EKE (59% ± 3%, n = 8) as compared to wildtype (37 ± 5%, n = 8; $p < 0.01$, unpaired t-test; Fig. 1D).

We also investigated the effects of acidosis (pH 6.4) on steady-state fast inactivation of Nav1.7 and Nav1.7-EKE. 50 ms long pre-pulses ranging from −120 to −10 mV in steps of 10 mV were applied prior to the 20 ms long test-pulse to 0 mV. As shown in Fig. 1E, acidification leads to a non-significant leftward shift from V1/2–81 ± 0.4 mV (n = 7) at pH 7.4 to V1/2–80 ± 0.3 mV (n = 7) at pH 6.4 for the wildtype channel. While the voltage-dependency of fast inactivation was strongly shifted for hNav1.7-EKE at pH 7.4 (V1/2–61 ± 0.1 mV, n = 8) as compared to wildtype, application of pH 6.4 failed to induce a significant shift (V1/2–64 ± 1.0 mV, n = 8; Fig. 1F). Due to a very poor functionality of the hNav1.7-EKE construct, we refrained from performing a more detailed functional analysis.

3.2. Differences in proton sensitivity among α-subunits

Our data on hNav1.7-EKE correlate with the report from Smith et al. in regard to proton-sensitivity [18]. Similar to what is demonstrated in the report from Smith and colleagues, our

experiments also suffered from a very poor functionality of this mutant construct. We therefore sought an alternative way to further explore the relevance of the charge of the proposed motif protons on α-subunits. A sequence alignment on different mammalian α-subunits clearly indicated that the motif is not conserved in any way (Fig. 2A). Calculating the total charge of the corresponding three amino acids in each α-subunit revealed that hNav1.7 is the only α-subunit carrying a positively charged motif (++0, Fig. 2A). While hNav1.5 and rNav1.8 carry neutral motifs, rNav1.2, rNav1.3, rNav1.4 and mNav1.6 all carry a negatively charged motif like ANMrNav1.7. Thus if this motif is indeed relevant for protoninduced block across all α-subunits, we reasoned that the total charge should correlate with proton-sensitivity. We therefore explored tonic block of all these α-subunits by increasing concentrations of protons (Fig. 2B and C). Except for Nav1.6 and Nav1.8, all α-subunits were explored in HEK 293 cells. As both Nav1.6 and Nav1.8 fail to functionally express in HEK 293 cells, they were examined in the neuroblastoma cell line N1E115 in presence of 300 nM TTX (see also methods for details). The calculated Ki values for proton-evoked tonic block revealed discrete differences between the α-subunits (Fig. 2D): hNav1.7 (5.8 ± 0.05, Hill coefficient 1.1 ± 0.06, n = 8) < Nav1.4 (6.0 ± 0.05, Hill coefficient 1.04 ± 0.08, n = 7) = Nav1.5 (6.0 ± 0.02, Hill coefficient 1.1 ± 0.04; n = 8) < Nav1.2 (6.1 ± 0.02, Hill coefficient 1.06 ± 0.01, n = 7) = Nav1.3 (6.1 ± 0.02, Hill coefficient 1.07 ± 0.02, n = 7) < Nav1.6 (6.2 ± 0.08, Hill coefficient 1.02 ± 0.06; n = 12) = Nav1.8 (6.2 ± 0.05, Hill coefficient 1.04 ± 0.1, n = 6). Again, we also examined the degree of block induced by pH 6.0 only. Wildtype Nav1.7 was blocked by 37 ± 5% (n = 8) whereas all other α-subunits except for Nav1.4 (46 ± 5%, n = 6) exhibited a stronger block: Nav1.2: 59 ± 3% (n = 7), Nav1.3: 60 ± 2% (n = 7), Nav1.8 (61 ± 6%) and Nav1.6: 65 ± 3% (n = 11) (Fig. 2E) (one-way ANOVA with Fischer post-hoc test). When comparing the degree of block of hNav1.7-EKE with the other α-subunits however, no significant differences were determined. Furthermore, we could not determine a clear difference between α-subunits carrying a neutral motif (i.e. Nav1.5 and Nav1.8) as compared to those with a negatively charges motif (i.e. Nav1.2, Nav1.3, Nav1.4 and Nav1.6). We finally examined the acid-sensitivity of endogenous Na+

currents in the neuroblastoma cells ND7/23. It was previously demonstrated that these cells preferentially express Nav1.3 and Nav1.7 [11], and thus we expected that the acid-sensitivity of Na+ currents in these cells should lie between those determined for recombinant Nav1.3 and Nav1.7 channels. Indeed, tonic block of Na+ currents in ND7/23 cells revealed a Ki of 6.0 ± 0.03 (n = 7, Fig. 3A and B). Furthermore, block by 6.0 was 46 ± 3% in ND7/23 cells.

3.3. Location of the KKV motif in hNav1.7

The KKV residues are located on the S5–S6 extracellular linker that comprises the domain IV P-loop (Fig. 4A). The KKV motif is located 20 residues C-terminal to the alanine of the selectivity filter 'DEKA' residues and 17 residues C-terminal to the aspartate of the outer carboxylate ring of residues (sequence 'EETD' in hNav1.7) that also lines the pore mouth [9] (Fig. 4A). A homology model of hNav1.7 was generated based on the NavPaS channel from Periplaneta Americana, which represents the first eukaryotic voltage-gated sodium channel structure solved to high-resolution to date [16]. Fig. 4B shows the alignment used for generating the DIV S5, S6 and P-loop sections. Although the KKV motif is not found in NavPaS, the DEKA alanine, the DIV aspartate of the carboxylate ring and a pair of cysteine residues are conserved between these two channel sequences. These cysteines form a disulphide bond in the NavPaS structure and in the hNav1.7 model the KKV residues are located in the intervening loop region. Consequently the KKV motif is located on the periphery of the extracellular surface and over 20 Å from the carboxylate ring and selectivity filter residues that form the deepest and most constricted region of the pore mouth (Fig. 4C).

Discussion

In the present in vitro study we challenge a previously published report claiming that proton-evoked block of VGSC α-subunits depends on the charge of motif consisting of three amino acids within the P-loop of domain IV [18]. Although the proposed motif might thus be a relevant interaction site for protons on α-subunits, we are not aware of any follow up study that could verify the original report.

We find that the mutant construct hNav1.7-EKE, which resembles the highly proton-sensitive Nav1.7 orthologue of the African naked mole indeed displays an increased tonic block by protons as compared to wildtype hNav1.7 channels. However, the validity of our experiments might be limited due to the strongly reduced functionality of the mutant construct. This was not only observed by very small peak current amplitudes in most investigated cells, but also by a strongly altered voltage-dependency of fast inactivation. Although this loss of function of the Nav1.7-EKE construct was not mentioned in the original report from Smith et al., the depicted current traces with very small inward currents in their report indeed indicate that their construct also suffered from a profound loss of function [18]. As such strong functional deficits might result in unspecific pharmacological changes, we sought to employ an alternative approach to explore whether or not the motif charge dictates proton-evoked tonic block. Instead of creating further mutated α-subunits which possibly also display a similar loss of function phenotype, we reasoned that the relevance of the proposed motif for proton-evoked block should be similar in most if not all α-subunits. To our surprise, the sequence alignment on the α-subunits examined in our study revealed that the motif is not conserved among different to αsubunits to any degree. Thus neither did we determine conserved residues among the three amino acids, nor was the total charge of this motif conserved.

When looking at Nav1.7 from different mammalian species however, it is evident that the negatively charged motif in the African naked mole rat (EKE) is also found in several other

hibernating mammals which putatively all live in acidic environments [12]. On the other hand, the double-positive charge of the motif in human Nav1.7 (KKV) is conserved in the Nav1.7 orthologues of several higher developed mammalian species [12]. While a motif with an overall positive (or even double-positive) charge is not found in any other α-subunit than in Nav1.7, we found that several α-subunits carry negatively charged motifs. While we could not identify a clear association between a negative charge of the motif and a high proton-sensitivity, the positive charge in Nav1.7 was associated with a low proton-sensitivity. This association may be purely due to a coincidence, but our data strongly question the previously postulated one directed hypothesis that the negatively charged motif of Nav1.7 in hibernating mammals is likely due to evolutionary pressure. When considering our data, it seems more appropriate to speculate about the possibility that the positive charge of Nav1.7 in many higher developed mammals may due to evolutionary pressure aiming to secure an intact pain sensitivity under acidic conditions and also acid-evoked pain. There is little doubt that Nav1.7 is crucial for pain sensitivity in at least humans and rodents [3], and thus the comparably low proton-sensitivity of Nav1.7 as compared to the other α-subunits may reflect that ability of human and rodent nociceptors to remain functional even at extremely acidic conditions.

In our experiments Nav1.7 was more resistant against block by protons than Nav1.8 which is also generally considered a key α-subunit for excitability of nociceptors under various conditions [15]. This finding correlates well the reports from Nakamura and colleagues, demonstrating that in rat dorsal root ganglion neurons TTX-sensitive Na+ currents (which are predominantly generated by Nav1.7) display less proton-evoked block as compared to TTX-resistant Na+ currents (i.e. Nav1.8 and Nav1.9) [13,14]. Our data also suggest that the skeletal muscle α-subunit Nav1.4 is relatively resistant towards block by protons as compared to several other α-subunits. As Nav1.4 carries a negatively charged motif, this finding speaks against a general role of this motif for proton-evoked block in all α-subunits. In agreement with our data on Nav1.4 however, Khan et al. found that Nav1.4, but not Nav1.5 generate a proton-resistant Na+ current even at strong acidosis (pH 5.0) and postulated that this may secure activation of skeletal muscle during acidosis [8,9]. The authors found that the

TTX-binding site located in the selectivity filter (in Nav1.5: Cystein373) is partly dictating this subunit-specific difference, thus proposing another not yet verified motif for protons on α-subunits [8]. Nevertheless, a relative resistance towards modification by acidosis was also found for Nav1.4 when compared to Nav1.2 and Nav1.5 [20]. Thus their seem to be relevant αsubunit-specific differences in regard to proton-sensitivity, and so far relatively little is known about which targets or motifs for protons are relevant. The data in our study at least suggest that human Nav1.7 displays a very low proton-sensitivity as compared to many other αsubunits, and this property may be due to its important role for the excitability of nociceptors also as acidic conditions.

The structure of NavPaS revealed the arrangement of the selectivity filter and outer carboxylate ring of the pore mouth and also the numerous disulphide bridges that are proposed to stabilize the structure of the P-loops [16]. Two cysteines that form a disulphide bond in the NavPaS DIV P-loop are also conserved in human and naked mole rat Nav1.7 sequences and indeed in all human isotypes, suggesting an underlying structural conservation. The KKV residues (and the corresponding EKE residues of the naked mole rat) are located on the loop region bound by this disulphide on the periphery of the extracellular surface. Given how distal the KKV motif is from the pore mouth, it seems unlikely that the charge and ionization state of these residues would affect channel conductance by means of altered electrostatic interactions with ions [18]. Instead, substitutions at the KKV motif may affect ion conductance through an as yet unknown allosteric effect on the channel structure.

References

[1] C.S. Bond, A.W. Schuttelkopf, ALINE: a WYSIWYG protein-sequence alignment editor for publication-quality alignments, Acta Crystallogr. D: Biol Crystallogr. 65 (2009) 510–512, http://dx.doi.org/10.1107/S0907444909007835.

[2] J. de la Roche, M.J. Eberhardt, A.B. Klinger, N. Stanslowsky, F. Wegner,

W. Koppert, P.W. Reeh, A. Lampert, M.J. Fischer, A. Leffler, The molecular basis for species-specific activation of human TRPA1 protein by protons involves poorly conserved residues within transmembrane domains 5 and 6, J. Biol. Chem. 288 (2013) 20280–20292, http://dx.doi.org/10.1074/jbc.M113.479337.

[3] S.D. Dib-Hajj, Y. Yang, J.A. Black, S.G. Waxman, The Na(V)1.7 sodium channel:

from molecule to man, Nat. Rev. Neurosci. 14 (2013) 49–62, http://dx.doi.org/10.

1038/nrn3404.

[4] N. Eswar, B. Webb, M.A. Marti-Renom, M.S. Madhusudhan, D. Eramian, M.Y. Shen, U. Pieper, A. Sali, Comparative protein structure modeling using MODELLER, Curr. Protoc. Protein Sci. (2007) ps0209s50, http://dx.doi.org/10.1002/0471140864

Chapter 2: Unit 2–9.

[5] J.G. Hoeijmakers, C.G. Faber, I.S. Merkies, S.G. Waxman, Painful peripheral neuropathy and sodium channel mutations, Neurosci. Lett. 596 (2015) 51–59, http:// dx.doi.org/10.1016/j.neulet.2014.12.056.

[6] P. Holzer, Acid-sensitive ion channels and receptors, Handb. Exp. Pharmacol. (2009) 283–332, http://dx.doi.org/10.1007/978-3-540-79090-7_9.

[7] D.K. Jones, P.C. Ruben, Proton modulation of cardiac I Na: a potential arrhythmogenic trigger, Handb. Exp. Pharmacol. 221 (2014) 169–181, http://dx.doi. org/10.1007/978-3-642-41588-3_8.

[8] A. Khan, J.W. Kyle, D.A. Hanck, G.M. Lipkind, H.A. Fozzard, Isoform-dependent interaction of voltage-gated sodium channels with protons, J. Physiol. 576 (2006)

493–501, http://dx.doi.org/10.1113/jphysiol.2006.115659.

[9] A. Khan, L. Romantseva, A. Lam, G. Lipkind, H.A. Fozzard, Role of outer ring carboxylates of the rat skeletal muscle sodium channel pore in proton block, J. Physiol. 543 (2002) 71–84.

[10] A. Leffler, B. Monter, M. Koltzenburg, The role of the capsaicin receptor TRPV1 and

acid-sensing ion channels (ASICS) in proton sensitivity of subpopulations of primary nociceptive neurons in rats and mice, Neuroscience 139 (2006) 699–709, http://dx. doi.org/10.1016/j.neuroscience.2005.12.020.

[11] A. Leffler, J. Reckzeh, C. Nau, Block of sensory neuronal Na+ channels by the secreolytic ambroxol is associated with an interaction with local anesthetic binding sites, Eur. J. Pharmacol. 630 (2010) 19–28, http://dx.doi.org/10.1016/j.ejphar.

2009.12.027.

[12] Z. Liu, W. Wang, T.Z. Zhang, G.H. Li, K. He, J.F. Huang, X.L. Jiang, R.W. Murphy, P. Shi, Repeated functional convergent effects of NaV1.7 on acid insensitivity in hibernating mammals, Proc. Biol. Sci. 281 (2014) 2013295, http://dx.doi.org/10.

1098/rspb.2013.2950.

[13] M. Nakamura, I.S. Jang, Acid modulation of tetrodotoxin-resistant Na(+) channels in rat nociceptive neurons, Neuropharmacology 90 (2015) 82–89, http://dx.doi. org/10.1016/j.neuropharm.2014.11.005.

[14] M. Nakamura, D.Y. Kim, I.S. Jang, Acid modulation of tetrodotoxin-sensitive Na+ channels in large-sized trigeminal ganglion neurons, Brain Res. 1651 (2016) 44–52, http://dx.doi.org/10.1016/j.brainres.2016.09.019.

[15] A.M. Rush, T.R. Cummins, S.G. Waxman, Multiple sodium channels and their roles in electrogenesis within dorsal root ganglion neurons, J. Physiol. 579 (2007) 1–14, http://dx.doi.org/10.1113/jphysiol.2006.121483.

[16] H. Shen, Q. Zhou, X. Pan, Z. Li, J. Wu, N. Yan, Structure of a eukaryotic voltagegated sodium channel at near-atomic resolution, Science 355 (2017), http://dx.doi. org/10.1126/science.aal4326.

[17] F. Sievers, A. Wilm, D. Dineen, T.J. Gibson, K. Karplus, W. Li, R. Lopez,

H. McWilliam, M. Remmert, J. Soding, J.D. Thompson, D.G. Higgins, Fast, scalable generation of high-quality protein multiple sequence alignments using Clustal Omega, Mol. Syst. Biol. 7 (2011) 539, http://dx.doi.org/10.1038/msb.2011.75.

[18] E.S. Smith, D. Omerbasic, S.G. Lechner, G. Anirudhan, L. Lapatsina, G.R. Lewin, The molecular basis of acid insensitivity in the African naked mole-rat, Science 334 (2011) 1557–1560, http://dx.doi.org/10.1126/science.1213760.

[19] C. Stoetzer, K. Kistner, T. Stuber, M. Wirths, V. Schulze, T. Doll, N. Foadi,

F. Wegner, J. Ahrens, A. Leffler, Methadone is a local anaesthetic-like inhibitor of neuronal Na+ channels and blocks excitability of mouse peripheral nerves, Br. J. Anaesth. 114 (2015) 110–120, http://dx.doi.org/10.1093/bja/aeu206.

[20] Y.Y. Vilin, C.H. Peters, P.C. Ruben, Acidosis differentially modulates inactivation in na(v)1.2, na(v)1.4, and na(v)1.5 channels, Front. Pharmacol. 3 (2012) 109, http:// dx.doi.org/10.3389/fphar.2012.00109.

[21] L. Willard, A. Ranjan, H. Zhang, H. Monzavi, R.F. Boyko, B.D. Sykes, D.S. Wishart, VADAR: a web server for quantitative evaluation of protein structure quality, Nucleic Acids Res. 31 (2003) 3316–3319.

Acknowledgements

The authors gratefully acknowledge the assistance of Heike Bürger and Kerstin Reher (Anesthesiology, Hannover).

Figure legends

Figure 1

Tonic block and steady state fast inactivation of Nav1.7 and Nav1.7-EKE by acidosis

A and **B**. Tonic block of Na^+ currents by protons in cells expressing wildtype human Nav1.7 (A) or Nav1.7-EKE (B). Cells were held at -120 mV and solutions with decreasing pH-values were applied. **C**. Concentration-dependent tonic block of wildtype Nav1.7 (black squares) and Nav1.7-EKE (red circles) by acidosis. Peak amplitudes of Na^+ currents at different pH-values were normalized with respect to the peak amplitude at pH 7.4. Data were fitted with the Hill equation represented by the solid line. **D.** Bar diagram depicting the average Na^+ current reduction following application of pH 6.0 in cells expressing wildtype Nav1.7 or Nav1.7-EKE. **E** and **F**. Voltage-dependency of fast inactivation of wildtype Nav1.7 (E) and Nav1.7-EKE (F) at pH 7.4 and pH 6.4. Fast inactivation was induced by 50 ms long pre-pulses ranging from -120 mV to -10 mV in steps of 5 mV, and the remaining fraction of available channels was examined with a 20 ms long pre-pulse to 0 mV. Solid lines represent fits obtained with the Boltzmann equation. Errors bars represent mean ± S.E.M.

Figure 2

α-subunit-specific tonic inhibition by protons

A. Sequence alignment within domain IV highlighting the amino acids proposed to form a relevant motif for proton-induced block. The charges of the individual amino acids within each motif are noted in the red frame. **B** and **C**. Tonic block of Na^+ currents by protons in cells expressing Nav1.3 (B) or Nav1.8 (C). **D.** Concentration-dependent tonic block of different □-subunits by acidosis. Peak amplitudes of Na^+ currents at different pH-values were normalized with respect to the peak amplitude at pH 7.4. Data were fitted with the Hill equation represented by the solid line. **E.** Bar diagram depicting the average Na^+ current reduction following application of pH 6.0 in cells expressing different □-subunits. * indicates a

significant difference as compared to Nav1.7. n.s. indicates a not significant difference between Nav1.4 and Nav1.7. Errors bars represent mean ± S.E.M.

Figure 3

A. Tonic block of Na^+ currents by protons in ND7/23 cells. Cells were held at -120 mV and solutions with decreasing pH-values were applied. **B**. Concentration-dependent tonic block of Na^+ currents in ND7/23 cells by acidosis. Peak amplitudes of Na^+ currents at different pH-values were normalized with respect to the peak amplitude at pH 7.4. Data were fitted with the Hill equation represented by the solid line.

Figure 4

Location of the 'KKV' sequence motif in hNav1.7.

A. Transmembrane topology map showing residues of the selectivity filter ('DEKA'; brown circles), outer carboxylate ring ('EETD'; purple circles), cysteines in the DIV P-loop ('CC'; orange circles) and the 'KKV' sequence (red circles). **B**. Sequence alignment showing the 'KKV' sequence (red background) of hNav1.7 and the conserved cysteines (orange background) that form a disulphide bond in the DIV P-loop of the NavPaS structure. Helices in the NavPaS structure are depicted as cartoons **C.** Nav1.7 homology model coloured by chain showing the selectivity filter DEKA residues (brown spheres), outer carboxylate ring (purple spheres), DIV P-loop disulphide bond (orange spheres) and 'KKV' residues (red spheres).

Figure 1

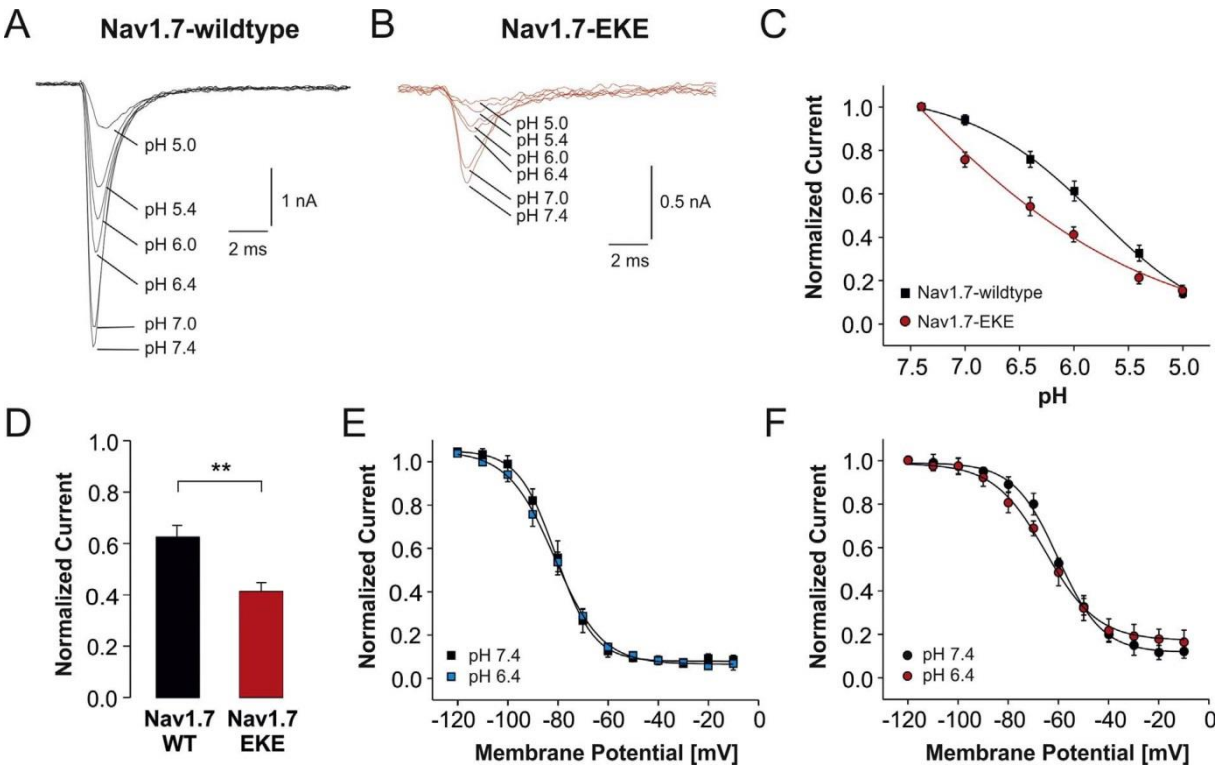
A
Nav1.7-wildtype
pH 5.0
pH 5.4
pH 6.0
pH 6.4
pH 7.0
pH 7.4
1 nA
2 ms
B
Nav1.7-EKE
pH 5.0
pH 5.4
pH 6.0
pH 6.4
pH 7.0
pH 7.4
0.5 nA
2 ms
C
Normalized Current
Nav1.7-wildtype
Nav1.7-EKE
pH
D
Normalized Current
**
Nav1.7 WT
Nav1.7 EKE
E
Normalized Current
pH 7.4
pH 6.4
Membrane Potential [mV]
F
Normalized Current
pH 7.4
pH 6.4
Membrane Potential [mV]

Figure 2

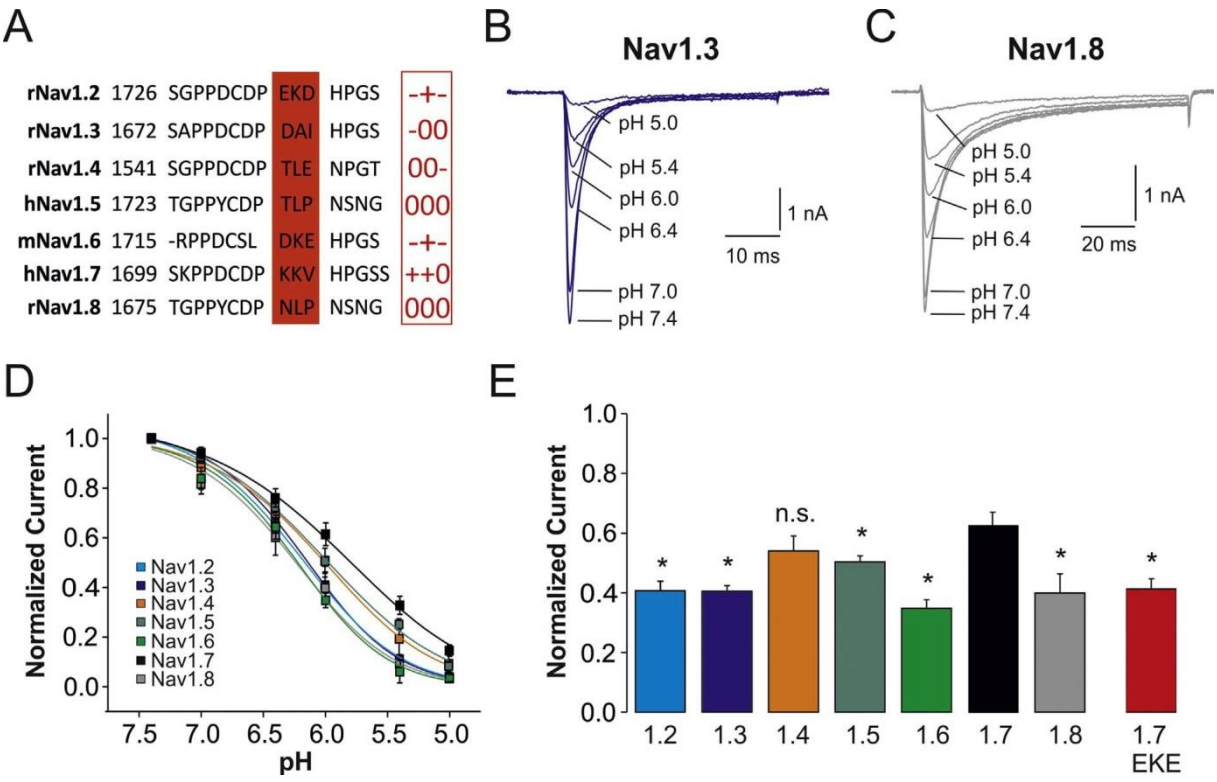
A
rNav1.2 1726 SGPPDCDP EKD HPGS -+-
rNav1.3 1672 SAPPDCDP DAI HPGS -00
rNav1.4 1541 SGPPDCDP TLE NPGT 00-
hNav1.5 1723 TGPPYCDP TLP NSNG 000
mNav1.6 1715 -RPPDCSL DKE HPGS -+-
hNav1.7 1699 SKPPDCDP KKV HPGSS ++0
rNav1.8 1675 TGPPYCDP NLP NSNG 000
B
Nav1.3
pH 5.0
pH 5.4
pH 6.0
pH 6.4
pH 7.0
pH 7.4
1 nA
10 ms
C
Nav1.8
pH 5.0
pH 5.4
pH 6.0
pH 6.4
pH 7.0
pH 7.4
1 nA
20 ms
D
Normalized Current
1.0
0.8
0.6
0.4
0.2
0.0
Nav1.2
Nav1.3
Nav1.4
Nav1.5
Nav1.6
Nav1.7
Nav1.8
7.5 7.0 6.5 6.0 5.5 5.0
pH
E
Normalized Current
1.0
0.8
0.6
0.4
0.2
0.0
n.s.
*
1.2 1.3 1.4 1.5 1.6 1.7 1.8 1.7 EKE

Figure 3

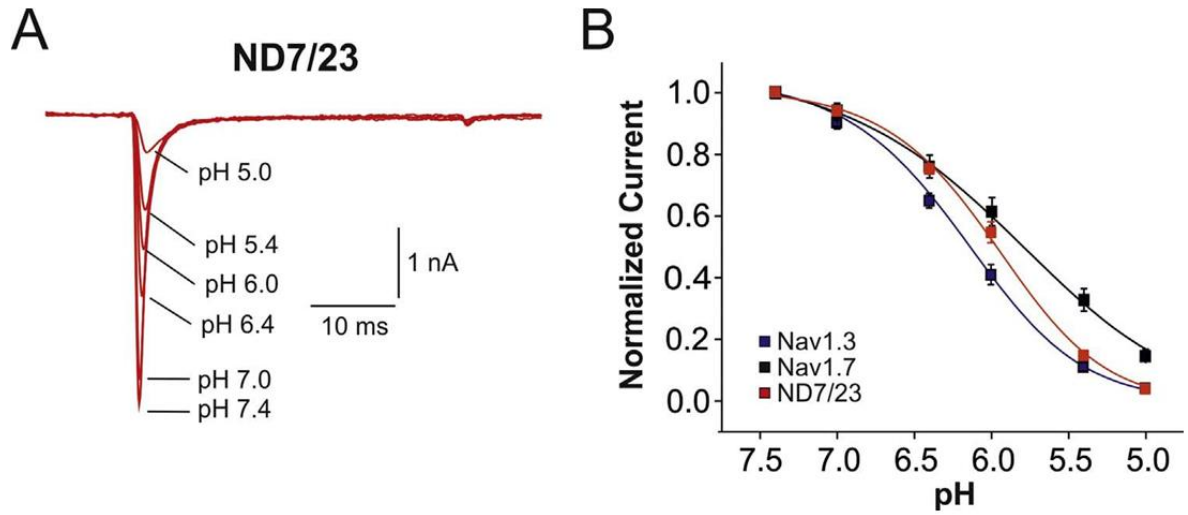
A
ND7/23
pH 5.0
pH 5.4
pH 6.0
pH 6.4
pH 7.0
pH 7.4
1 nA
10 ms
B
Normalized Current
1.0
0.8
0.6
0.4
0.2
0.0
Nav1.3
Nav1.7
ND7/23
7.5
7.0
6.5
6.0
5.5
5.0
pH

Figure 4

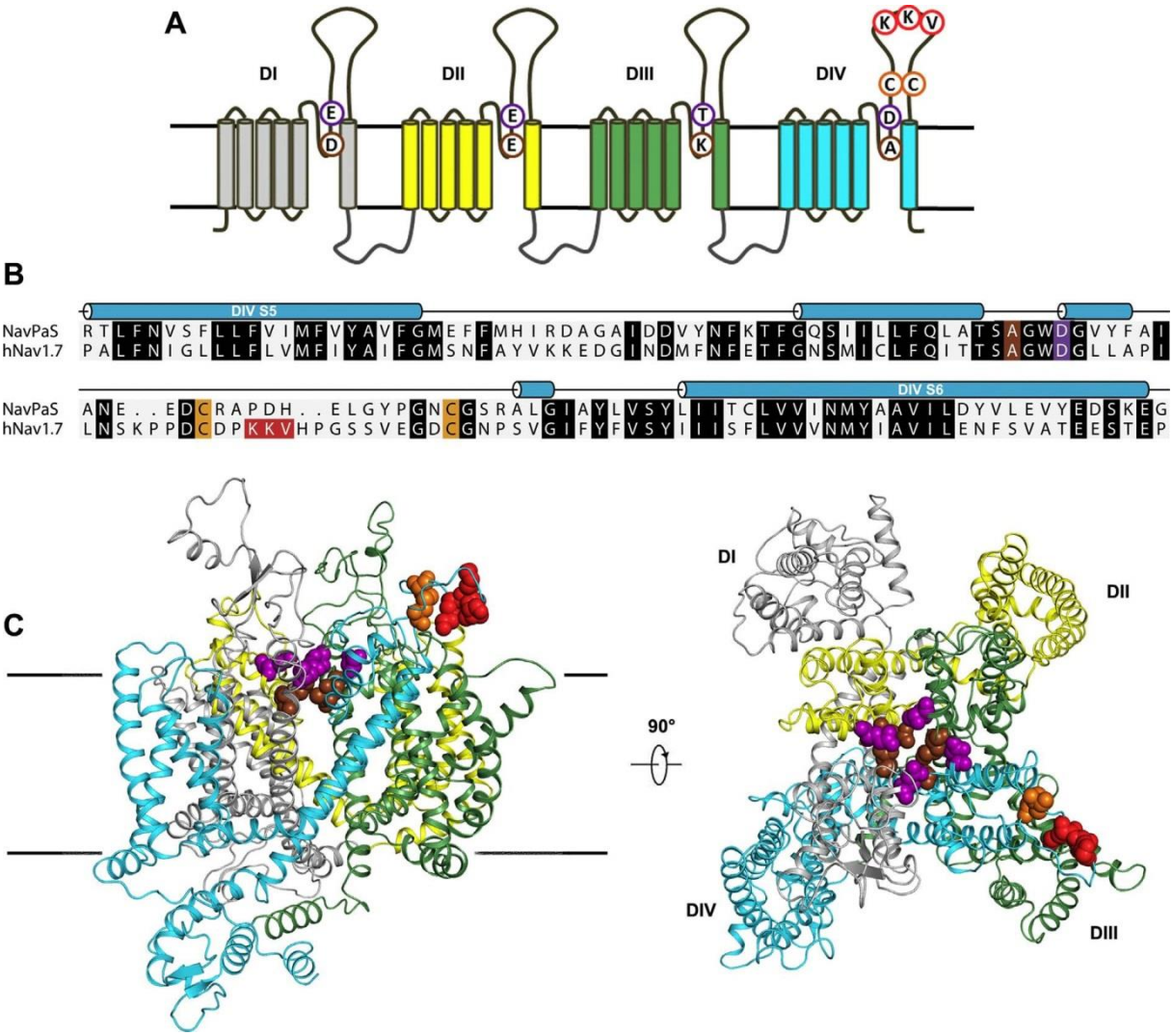
A
DI
DII
DIII
DIV
E
D
E
E
T
K
K
K
V
C
C
D
A
B
DIV S5
DIV S6
NavPaS RTLFNVSFLLFVIMFVYAVFGMEFFMHIRDAGAIDDVYNFKTFGQSIILLFQLATSAGWDGVYFAI
hNav1.7 PALFNIGLLLFLVMFIYAIFGMSNFAYVKKEDGINDMFNFETFGNSMICLFQITTSAGWDGLLAPI
NavPaS ANE..EDCRAPDH..ELGYPGNCGSRALGIAYLVSYLIITCLVVINMYAAVILDYVLEVYEDSKEG
hNav1.7 LNSKPPDCDPKKVHPGSSVEGDCGNPSVGIFYFVSYIIISFLVVVNMYIAVILENFSVATEESTEP
C
90°
DI
DII
DIV
DIII